FMCW Multiplexing of Fiber Bragg Grating Sensors

Peter K. C. Chan, Wei Jin, *Senior Member, IEEE*, and M. Süleyman Demokan, *Senior Member, IEEE*

***Abstract*—We report on the use of frequency-modulated continuous wave (FMCW) techniques for multiplexing fiber Bragg grating (FBG) sensors. This technique is based on the modulation of light intensity from a broadband source by a linear swept-frequency RF carrier. Signals from the FBG sensors located at different positions in an array are separated in frequency domain and demodulated using a tunable optical filter. The potential and limitation of the technique are discussed. A three-sensor FMCW multiplexed FBG array of parallel topology and a six-sensor hybrid FMCW/WDM system were experimentally demonstrated with −30 dB crosstalk between sensors and 2 $\mu\varepsilon$ resolution in terms of root mean square (RMS) strain value.**

***Index Terms*—Fiber Bragg grating sensors, frequency-modulated continuous wave, optical fiber sensors, strain measurements.**

I. Introduction

FIBER Bragg gratings (FBGs) have been identified as very important sensing elements, especially for strain measurements in smart structures [1]–[4]. In many applications, arrays of FBG sensors are required for multipoint or quasidistributed measurements. Multiplexing of FBG sensors is therefore essential in order to reduce the cost per sensing point and to increase the competitiveness of FBG sensors against conventional electrical sensors.

The most popular technique for multiplexing FBG sensors is the wavelength division multiplexing (WDM) technique [4], [5]. The maximum sensor number that can be multiplexed using the WDM technique is determined by the ratio of the source spectral width over the spacing between the Bragg wavelengths of the FBGs. For applications requiring a larger multiplexing gain, a combination of the WDM and time-division multiplexing (TDM) techniques [3]–[5] may be used.

A TDM system employs a pulsed or gated CW source to illuminate gratings in sequence as the pulse travels along the fiber, the reflected signals from the gratings are separated in time domain [6]. The physical separation between the gratings is determined by the input pulse width. A fast time-gated photodetector can be used to select the signal from individual grating for analysis. To achieve a large multiplexing gain without sacrificing the SNR, narrow optical pulses with relatively large peak power and hence large bandwidth of photodetector are required. The maximum sensor numbers is in general limited to less than ten.

A code-division multiple access (CDMA) scheme has recently been demonstrated for dense wavelength division multiplexing of FBG sensors [7]. The CDMA technique has a higher duty cycle and therefore larger average sensor output power over the TDM technique and consequently better SNR. For the same level of source power, the sensor number limited by input power level for CDMA could be significantly larger than that for TDM. The sensor number and channel isolation are proportional to the sequence lengths of the code sequence. Although a large number of FBGs were expected by use of CDMA technique, only a two sensor system was experimentally demonstrated with a crosstalk level of ∼20 dB [7].

The FMCW technique has been studied for multiplexing intensity-based [8] and interferometric fiber optic sensors [9]–[11]. This idea is extended here to address an array of FBG sensors that have approximately the same Bragg wavelength. The high duty cycle available using the FMCW technique provides a larger average power at the photo-detector and thus a better SNR. The FMCW technique can also be used in combination with the WDM technique to realize larger size FBG arrays.

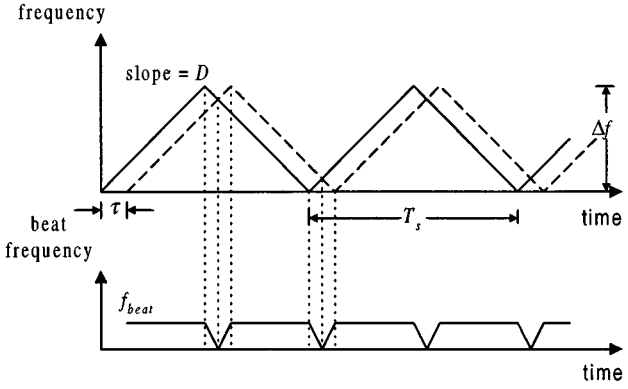

Fig. 1. Production of beat note.

II. Theory of FMCW

A. Principle of Operation

The basic theory of the FMCW technique has been described by Hymans *et al.* [12] and Manafza *et al.* [13]. Here we outline the pertinent factors and focus on the use of the technique for multiplexing FBG sensors.

Fig. 1 shows the concept of FMCW technique where a triangular frequency chirping is assumed. A time difference between a triangular chirped reference waveform and a signal (a delayed version of the reference) produce a difference frequency (beat frequency $f_{\rm beat}$) proportional to the rate of frequency excursion D and the time difference between two waves τ, i.e. $f_{\rm beat} = D\tau$. For a periodic frequency chirping of period T_s or repetition rate $f_s = 1/T_s$, the resultant output is of a line spectrum at intervals of f_s. The position of the peak in the envelope of the line spectrum gives the beat frequency $f_{\rm beat}$.

Manuscript received March 14, 2000; revised August 1, 2000. This work was supported by a Hong Kong Polytechnic University Research Grant (Project V-390).

The authors are with the Department of Electrical Engineering, Hong Kong Polytechnic University, Hung Hom, Kowloon, Hong Kong (e-mail: eekcchan@ee.polyu.edu.hk).

Publisher Item Identifier S 1077-260X(00)11236-5.

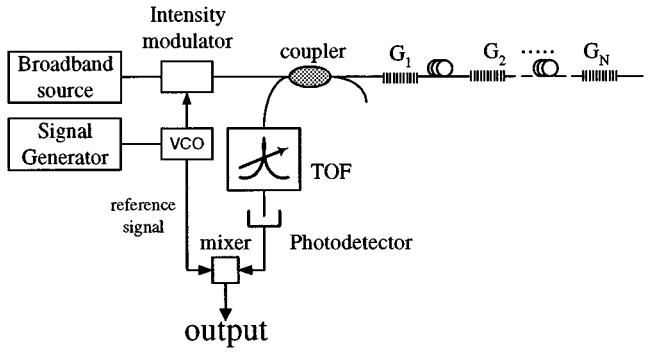

Fig. 2. Schematic diagram of an FMCW multiplexed FBG sensor array in serial topology.

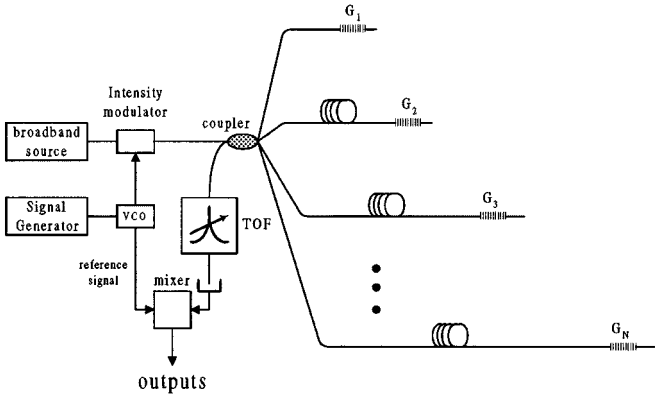

Fig. 3. Schematic diagram of an FMCW multiplexed FBG sensor array in parallel topology.

Figs. 2 and 3 show, respectively, a serial and a parallel FBG sensor array that are addressed by FMCW technique. The FBGs in the array can have either identical or different Bragg wavelengths. The light from the broadband source is modulated with a sawtooth or triangular chirped frequency carrier generated from a voltage-controlled oscillator (VCO) and launched into the FBG sensor array. The reflected signals from FBGs are guided back to a tunable optical filter (TOF) and then to a photo-detector and are mixed with a reference signal from the VCO subsequently. The system output will consist of a number of beat notes with the beat frequencies determined by the time delay differences (τ_i, $i = 1, 2, \cdots, N$, corresponding to N sensors) between the reflected signals from individual FBG sensors and the reference signal. If τ_i is selected properly, the beat note signals may be separated in frequency domain and viewed by using an electrical spectrum analyzer or using FFT analysis of the time domain signal after photodetection. Electronic bandpass filters with appropriate passing band may also be used to separate signals from different sensors. The separated sensor signal has amplitude proportional to the convolution of the spectral response of the optical tunable filter and that of the specific FBG sensor. The Bragg wavelengths of the individual FBGs can therefore be interrogated by scanning the TOF and recording the control voltages of the TOF that corresponding to the peaks of the different frequency components.

For chirping repetition rate f_s and the frequency excursion Δf, the rate of frequency excursion is $D = 2f_s\Delta f$, and the beat frequency corresponding to the ith sensor may be written as

$$f_{\text{beat}_i} = D\tau_i = 2f_s\Delta f\tau_i \tag{1}$$

where τ_i is the time delay difference between the signal from the ith sensor, and the reference signal τ_i includes contributions to the fiber delay lines and the delay introduced by the optoelectronic components such as the intensity modulator, the TOF and the photodetector.

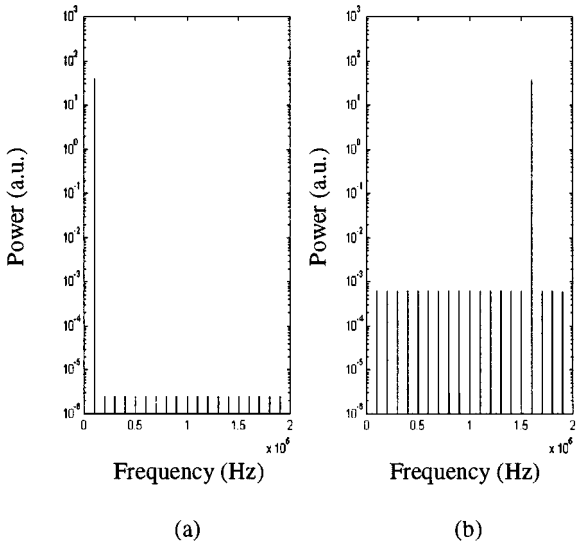

Fig. 4. Simulated beat note spectrum. (a) $\tau = 25$ ns and (b) $\tau = 400$ ns.

B. Beat Notes Spectrum

For triangular frequency chirping, the spectrum of the beat note corresponding to a particular sensor consists of a group of discrete lines with f_s interval and a sinc-function envelope. The exact spectral characteristics of the beat notes are complex and depend on a number of parameters, including the delay time τ between the sensor and the reference signals, the chirping repetition rate f_s and the frequency excursion Δf. Under the condition that

$$f_{\text{beat}} = kf_s \quad \text{or} \quad 2\Delta f\tau = k \tag{2}$$

i.e., the beat frequency coincides with one of the harmonics of f_s, the kf_s component will be maximized and other harmonics components would be near the minima of the sinc function. This means that the spectrum of the beat note may be approximately regarded as a single line if the aforementioned conditions are satisfied. Computer simulations have been conducted to show the effect of varying the parameters τ and T_s on the spectral characteristics of the beat note spectrum. Fig. 4 shows the simulation results for $\Delta f = 40$ MHz, $f_s = 5$ kHz, and $\omega_o = 2\,\pi\,80 \times 10^6$ rads. These are the values used in our experimental study that will be used throughout the paper. In Fig. 4(a), the delay difference τ was chosen to be $\tau = 25$ ns that satisfies $2\Delta f\tau = 2$. The ratio of the magnitudes of the peak to the first sideline is about -72 dB. The magnitudes of the sidelines increases with the value of k (proportional to τ) and reaches to about -48 dB for $k = 32$ or $\tau = 32/(2\Delta f) = 400$ ns (see

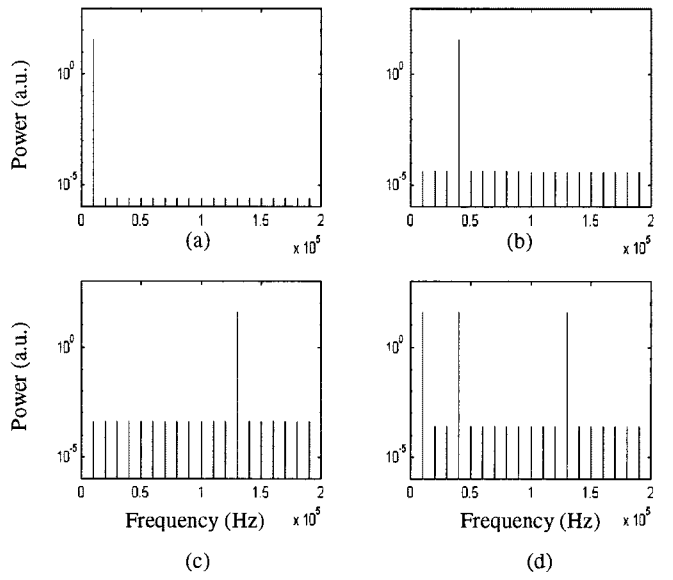

Fig. 5. Spectral lines of three individual sensors (a, b, c) and the combined signal (d).

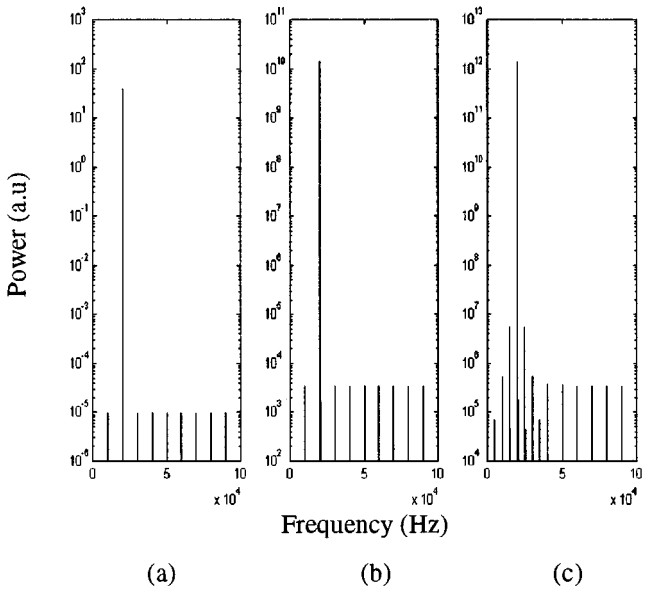

Fig. 6. Simulated beat note spectra ($f_{\rm beat} = 20$ kHz) for (a) a single reflector, (b) a 1-cm-long FBG, and (c) a 10-cm-long FBG.

Fig. 4(b). These results indicate that, if the sensor array is designed in such a way that each sensor signal aligns to a different harmonic of the frequency chirping, a maximum of 32 sensor may be multiplexed theoretically with crosstalk between any two of the sensors below −48 dB. The peak to sideline amplitude ratio depends not only on the time delay τ but also the modulating period T_s. The general trend is that the sideline suppression ratio will decrease with a decrease in τ or f_s.

For multiple sensor arrays as shown in Figs. 2 and 3, the output signal spectrum will be a superposition of individual sensor signals in the frequency domain. Fig. 5 shows the spectral lines of the combined signals from a three-sensor array [Fig. 5(d)] and the respective spectral lines of the individual sensors [Fig. 5(a)–(c)]. The time delay difference of the three sensors relative to the reference signal are 25 ns, 100 ns, and 325 ns, corresponding to $k = 2$, 8, and 26, respectively. It is interesting to note that the magnitude of the sidelines for the combined signal are actually smaller than that for the third sensor [Fig. 5(c), $k = 26$], indicating that the spectral components of the three sensors at a particular frequency (kf_s) are not always added in phase.

III. Performance Analysis of FMCW System

A. Effect of the Length of FBG

It should be mentioned that in obtaining the simulation results shown in Figs. 4 and 5, we have actually assumed that the sensor was a single reflector, i.e., each sensor has a unique time delay τ_i associated with it. In practice, an FBG cannot be regarded as a single reflector. This is because any FBG would have a limited length and may be modeled as a number of discrete reflectors connected in series, and each has a respective delay in relative to the reference signal and produces a unique set of beat notes. The beat notes corresponding to a FBG may be regarded as a superposition of a number of beat-notes signals produced by the reflectors.

The exact value of the sideline magnitude is difficult to obtain due to the complex distributed feedback nature of the FBG structure. A simple model is used here to estimate the upper limit of the sideline magnitude. An FBG is modeled as M reflectors connected in series ($M = L/\Lambda$, where L is the physical length of grating and Λ is the grating period, e.g., for a 1-cm-long 1550 nm FBG sensor, $M = 18\,840$). The power reflected from each of the reflectors is assumed to be the same. Fig. 6(a)–(c) show, respectively, the simulation results for a single reflector, a 1-cm-long FBG and a 10-cm-long FBG with the delay of the grating center corresponding to $2\Delta f\tau = 4(k = 4)$. For the 1-cm-long FBG, the magnitudes of the sidelines are 66 dB below the central peak, and it is very close (or may be regarded as the same) to that from the point reflector case [see Fig. 6(a)]. For the 10-cm-long FBG, the magnitudes of the sidelines are 54 dB below the peak line, indicating that the effect of the length of FBG sensors to the performance of FMCW system can be neglected.

B. Effect of Biasing from the Optimal Working Condition

On the other hand, the biasing from the optimal time delay difference τ may also affect the FMCW system performance. The beat note spectrum for a single sensor may be approximately regarded to be a single line, and the magnitude of the sidelines are essentially zero if the time delay τ and the modulation parameters Δf and f_s satisfy (2). In a multiplexed multiple sensor system, the modulation parameters are usually fixed to ensure that all the sensors in the network experience the same frequency chirping modulation. The only parameter that may be adjusted is the optical time delay difference τ. The time delay difference can be adjusted by a cutting and splicing technique or by directly writing FBGs on fibers in a controlled manner. For either technique, it should not be very difficult to control the separation between the FBGs to be within $\sim$1 cm accuracy or a time delay bias of $\tau = 2n\times$ (1 cm/c = 97 ps).

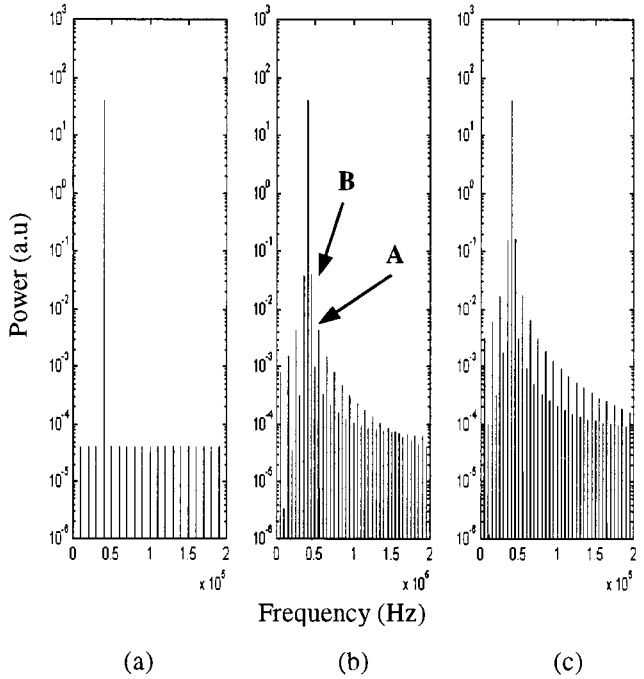

Fig. 7. Beat note spectrum of a sensor ($f_{\rm beat} = 40$ kHz) for (a) ideal case, (b) 1 cm longer than the optimal delay difference, and (c) 2 cm longer than the optimal delay difference.

To study the effect of biasing from the optimal condition, we carried out simulations for the set of modulation parameters given in Section II-B and for various time delays. Fig. 7(a)–(c) shows, respectively, the beat note spectra for three cases where the path difference between the sensor and the reference satisfying the optimal condition [i.e., (2) is satisfied with $k = 8$], 1 cm and 2 cm longer than the optimal condition. The magnitudes of the tallest (first pair of) sidelines are, respectively, 30 dB [Fig. 7(b)] and 24 dB [Fig. 7(c)] below the central peak. They are 30 dB and 36 dB above the sidelines, as shown in Fig. 7(a). It can be seen from Fig. 7(b) and (c) that the magnitudes of the sidelines reduce when they are further away from the main peak. Thus, for practical applications, the physical separation between the sensors may be made longer so that the adjacent sensor signal is located at a frequency line slightly further away from the peak, e.g., working at **A** line instead of **B** line. Crosstalk between sensors can then be reduced from -30 dB to -40 dB.

IV. Network Analysis

A. Spatial Separation Between the FBGs and the Maximum Sensor Number

An important conclusion drawn from Section II-B is that the time delay difference τ between the sensor signals and the reference signal should be ideally designed to be

$$\tau = \frac{k}{2\Delta f} \qquad k = 1, 2, 3, \cdots. \tag{3}$$

The magnitudes of the sidelines may be minimized provided that the aforementioned condition is satisfied. The nonzero sidelines would cause crosstalk between sensors. The minimum delay difference $\Delta\tau$ between sensors may be obtained by taking the derivative of (3), and expressed as

$$\Delta\tau = \frac{\Delta k}{2\Delta f} \tag{4}$$

where Δk is the difference in harmonic numbers. $\Delta\tau$ can be further expressed in terms of the fiber length difference ΔL between two gratings, the light velocity c and refractive index n

$$\Delta\tau = \frac{2\Delta L n}{c}. \tag{5}$$

Substituting (5) into (4), the minimum separation $\Delta L_{\min,1}$ between two adjacent sensors may be obtained by putting Δk to 1, as

$$\Delta L_{\min,1} = \frac{c}{4n\Delta f}. \tag{6}$$

Assume that $\Delta f = 40$ MHz, the time delay difference between sensors should be multiples of 12.5 ns. The physical separation should then be multiples of 1.25 m. The minimum separation $\Delta L_{\min,1}$ may be increased or reduced by varying Δf. However, the adjustment is limited due to the practical limit of the electronic devices (e.g., VCO) used.

The spatial separation between two neighboring FBGs is also affected by the spectral width of the FBGs and the TOF. The separation $\Delta L_{\min,2}$ between the gratings should be longer than the coherence length of the source, the equivalent coherence lengths of the FBG and the TOF, in order to avoid coherent interference to occur [14]. As the spectrum of a broadband source is usually much broader than that of FBGs and the TOF, the separation between the FBGs should be dictated by the equivalent coherence length L_c of the FBG or the TOF, whichever is larger, i.e.,

$$\Delta L_{\min,2} \gg L_c > \frac{{\lambda_B}^2}{B} \tag{7}$$

where λ_B is the Bragg wavelength of the grating, and $B = \min(B_G, B_F)$, B_G and B_F are the FWHM spectral width of the grating and the TOF, respectively.

For typical values, $\lambda_B \approx 1556$ nm and $B_G \approx B_F \approx 0.2$ nm, the value of L_c is 1.2 cm. For practical applications, the separation $\Delta L_{\min,2}$ may be chosen to be $10L_c = 12$ cm. This value may be the limiting value for this type of sensor arrays.

B. Power Budget Analysis

In order to balance the performance of the FBGs within the array, it is desirable to have equal reflected power from each of the FBG sensors. For the parallel architecture shown in Fig. 3, this can easily be done by choosing the FBGs in different branches to have identical peak reflectivity. For the serial FBG array shown in Fig. 2, the reflected light from different FBGs will not only depend on the peak reflectivity but also their relative Bragg wavelengths. If all the FBGs in the array have different Bragg wavelengths over the whole operation range, the returned power from different FBGs will be balanced if the FBGs are all of the same peak reflectivity. We are, however, interested here in multiplexing of FBGs of approximately the same Bragg wavelengths. For this type of

array, it is impossible to "balance" the power from different FBGs because the reflected power from the ith FBG depends on the Bragg wavelength of the first to the $(i-1)$th FBG, which depend on the measurand (strain) applied to the FBGs.

It may be however advantages to "balance" the power for the worse case where all the FBGs in the arrays are of the same Bragg wavelength. Consider now the serial FBG sensor array as shown in Fig. 2. As the power spectrum of broadband source is normally much broader than the tuning range of the grating, it may be assumed to have a constant spectrum power P_λ over this limited range. Assume the coupling ratio of the coupler is κ_c and the reflected peak power from ith FBG sensor G_i is given by

$$P_1 = (1-\kappa_c)\,\kappa_c {\alpha_T}^2 R_1 P_\lambda \qquad i=1 \tag{8}$$

$$P_i = (1-\kappa_c)\,\kappa_c \left[\prod_{j=1}^{i-1}(1-R_j)^2\right] {\alpha_T}^{2i} R_i P_\lambda \qquad i=2,3,\cdots,N \tag{9}$$

where $R_i (i=1,2,\cdots,N)$ denotes the peak reflectivity of the ith grating. α_T is the power transmission coefficient of the connecting fiber between the adjacent FBGs. For simplicity, the coefficients of all connecting fibers are assumed to be the same. Since the light intensity is modulated using a chirped frequency carrier, the average light power of the ith sensor will then be $P_i/2$.

Assume all the sensors have same reflected peak power, i.e., $P_i = P_{i+1}$. We have

$$R_i = (1-R_i)^2 {\alpha_T}^2 R_{i+1} \tag{10}$$

or

$$R_i = \frac{\left(2{\alpha_T}^2 R_{i+1}+1\right) - \sqrt{4{\alpha_T}^2 R_{i+1}+1}}{2{\alpha_T}^2 R_{i+1}}. \tag{11}$$

Once the reflectivity of the last FBG sensor in the array is known, the reflectivity of the other sensors and the corresponding reflected power at the photodetector can be calculated from (10) and (11) and (8) and (9), respectively.

As the number of sensors is increased, the optical power at the photodetector corresponding to each sensor will decrease. Since the photodetector has a minimum detectable optical power level, it will set a limit to the maximum number of sensors that can be multiplexed. Provided that we know the source spectral power P_λ and the noise equivalent power (NEP) of the photodetector, the maximum sensor number limited by power budget may be calculated by using (8)–(11). Take the New Focus 1811 photodetector as an example, for which the NEP is 2.5 pW/$\sqrt{\text{Hz}}$, and the bandwidth is 100 MHz. The minimum detectable power corresponding to an SNR ratio of 1 for that detector can be calculated to be -46 dBm. For an ASE source of power 15 mW, power level within the grating spectral region P_λ (say 0.2 nm linewidth) is about -12 dBm. Assume $\kappa_c = 0.5$ and $\alpha_T = 0.1$ dB, the power level of each sensor as a function of sensor number for a serial array (Fig. 2) was calculated from (8) and (9) and shown in Fig. 8. The four curves shown in the figure corresponds to $R_N = 1\%$ [curve (a)], 5% [curve (b)], 10% [curve (c)] and 100% [curve (d)], respectively. The maximum sensor number can be obtained from Fig. 8, by comparing the power level of the sensor with the minimum detectable power level of the detector, and are found to be 34, 52, 55, and 60 for $R_N =$ 1%, 5%, 10%, and 100%, respectively. The power level as a function of sensor number for a parallel array (Fig. 3) formed by using 2×2 fiber couplers and FBGs of 100% reflectivity are shown in Fig. 9. The maximum sensor number for SNR of 1 is 32. For practice applications, however, the SNR at the photodetector should be significantly larger than 1, e.g., SNR = 10. The maximum sensor number that can be multiplexed with the aforementioned source spectral power could be much less than the number mentioned above. Optical amplifiers may need to be used to boost up power level in order to multiplex a reasonable large number of sensors. Obviously, a larger number of sensors can be multiplexed with larger grating reflectivities. However, this may introduce larger crosstalk between sensors.

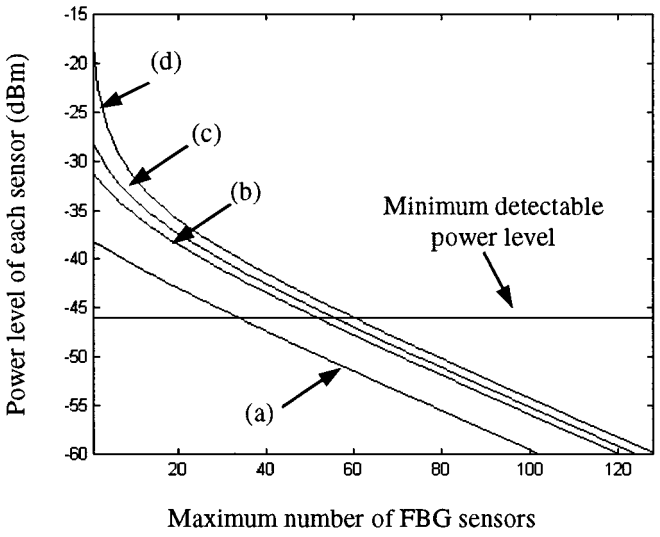

Fig. 8. Power level at the photodetector as function of the maximum number of FBG sensors in serial topology.

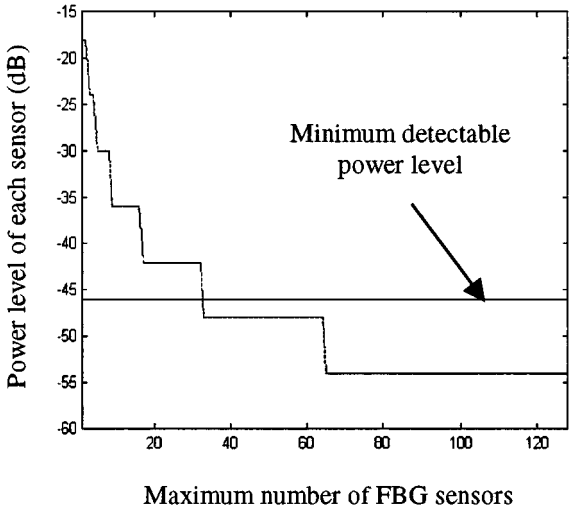

Fig. 9. Power level at the photodetector as function of the maximum number of FBG sensors in parallel topology.

C. Crosstalk Analysis

It has been shown in Section II-B that the crosstalk between sensors due to nonzero sidelines could be negligible if the beat frequency from a FBG sensor coincides with one of the harmonics of the modulating frequency f_s.

In a serial FBG array (Fig. 2), however, crosstalk may result from "Multiple-reflection" and "Spectral-shadowing" effects if the reflection spectra of two or more gratings are overlapping.

Multiple reflection between the gratings will generate residual reflected waves, which will produce residual beat signals in the output frequency spectrum. Some of the waves that travel similar distances with the grating signal may have a significant effect on the system performance. This crosstalk exists for any serial connected sensor array, no matter what type of address format (e.g. TDM, CDMA, or FMCW) is used. A detailed analysis of the effect of the multiple reflection on the crosstalk performance has been reported in [15].

The spectral shadowing crosstalk can be induced from upstream FBG sensors to downstream FBG sensors [16]. If the Bragg wavelengths of the gratings in the array are very close together, due to the spectral filtering effect of the upstream FBGs, the sensor signal from the downstream FBGs will be distorted. The measured peak wavelength of the downstream sensor would then be different from the real Bragg wavelength. The measurement error depends on the overlapping spectral content between the upstream FBGs and the FBG to be interrogated.

Both multiple reflection and spectral shadowing effects can be reduced by using low reflectivity gratings [15], [16]. However, the use of low reflectivity reduces the signal power of individual sensors at the output, thereby reducing the SNR. In order to maintain a reasonable power level at the photodetector, fiber amplifiers may need to be used before or after the sensor array to enhance the SNR.

Crosstalk from multiple reflection and spectral shadowing should not happen in a parallel topology system because the FBG sensors are located in different fiber branches, the light reflected from a particular sensor would not be influenced by other sensors.

V. Experiments and Results

The proof-of-principle experiment was reported in an earlier paper [18] where a three-sensor serial/parallel system was used. Here, we present more results on the experimental investigation of the FMCW technique.

A. Single Line Spectrum

A single grating system (Fig. 2, $N = 1$) was constructed to experimentally demonstrate the feasibility of obtaining a single line spectrum by matching the delay between the sensor and the reference signal to that of the harmonics of the repetition frequency. Before splicing the fiber with an FBG to the lead of the directional coupler, the length of the fiber was cut 1 cm at a step, and the output beat frequency spectrum was being monitored until the maximum of the beat note envelope was matched to one of the harmonics. An approximated single line spectrum with the magnitudes of sidelines of 38 dB below the central line

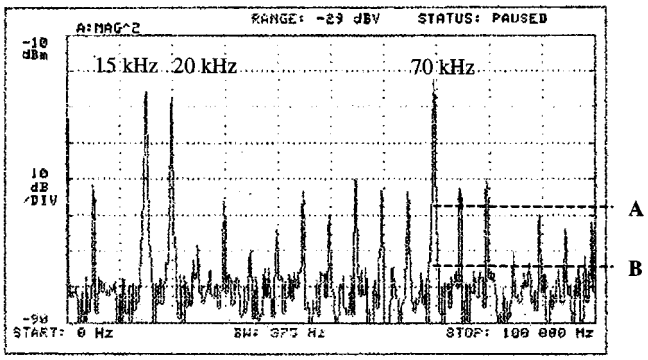

Fig. 10. Beat-note spectrum of the three-sensor system (**A**: magnitude of the line at 70 kHz when G_3 was not aligned to the TOF, **B**: magnitude of the line at 70 kHz when G_2 and G_3 were not aligned to the TOF).

was obtained by fine tuning the beat frequency to coincide with the third harmonic of the repetition frequency f_s. This indicates that crosstalk level between sensors could be below -38 dB if multiple sensors are multiplexed. This value of the central/sideline ratio (-38 dB) is believed to be limited by the nonideal response of the VCO used in our experiments.

B. Multiple FBG Sensors

A three-sensor system in parallel topology as shown in Fig. 3 ($N = 3$) was constructed and tested. The reflectivity of the FBG G_1, G_2, and G_3 are all approximately 100% and the Bragg wavelengths are 1547.68, 1548.36, and 1548.02 nm, respectively, at strain free condition. All gratings were secured on the transition stages. The frequency excursion was about 20 MHz. The physical separation between grating G_1 and G_2 is about 2.5 m, and the separation between G_1 and G_3 is about 13.8 m. All the gratings were strained so that they were aligned approximately to the TOF. The beat signals which displayed on an electrical spectrum analyzer are shown in Fig. 10. There are three major peaks in the spectrum display at 15 kHz, 20 kHz, and 70 kHz, corresponding to sensor G_1, G_2, and G_3, respectively. The sensor system has been tested for strain measurement. The measured control voltages of the TOF corresponding to the peaks of the beat signals show good linear relations with the applied strain, indicating no spectral-shadowing effect exist in the parallel sensor network. The strain resolution obtained was about $2\mu\varepsilon$ in terms of RMS strain value.

To investigate the crosstalk between sensors, the Bragg wavelength of G_3 was shifted away from the filter by applying strain and only G_1 and G_2 were aligned to the TOF. The magnitude of the sideline at 70 kHz was reduced from -24 dBm to -62 dBm (position **A** in Fig. 10). The corresponding crosstalk contributed from G_1 and G_2 to G_3 should then be -38 dB. The Bragg wavelength of G_2 was then shifted away by applying strain and only G_1 was aligned to the TOF. The sideline at 70 kHz was further decreased and almost reached the noise floor (position **B** in Fig. 10). At this circumstance, the crosstalk from G_1 and G_2 to G_3 can be neglected. Similar observations were made for lines at 15 kHz and 20 kHz for considering the crosstalk from G_2 and G_3 to G_1 and G_1 and G_3 to G_2 when G_1 and G_2 were not aligned to the TOF, respectively, the sidelines at 15 kHz and 20 kHz was 40 dB and 50 dB lower than that, showing in Fig. 10.

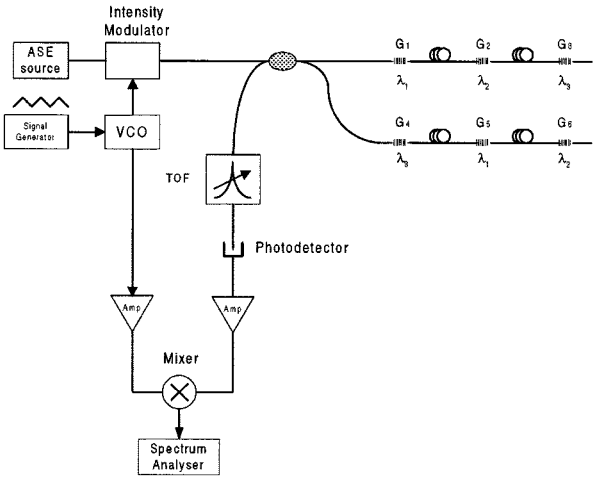

Fig. 11. Experiment setup of a hybrid FMCW/WDM system.

We also observed that the magnitudes of sidelines were not always increasing with the number of FBGs that were aligned to the TOF, indicating that the sidelines are not always added in phase. Therefore, we may conclude that the crosstalk level does not increase linearly with the number of FBG sensors in the FMCW system.

C. Hybrid FMCW/WDM System

The number of sensors can be increased by combining FMCW with WDM. An experimental setup of six-grating system was constructed as shown in Fig. 11. The reflectivity of the all FBGs is approximately 100% and the Bragg wavelengths are 1553.13 nm for G_1 and G_5, 1557.42 nm for G_2 and G_6 and 1562.78 nm for G_3 and G_4 at strain free condition. Each output arm from the coupler connected with three FBG sensors with different Bragg wavelengths. The sensors with the same Bragg wavelength were located in different arms and have their own beat frequencies that can be separated in frequency domain. The beat note spectra of G_1 and G_5, G_2 and G_6 and G_3 and G_4 are shown in Fig. 12 (a)–(c) respectively. The beat frequency of G_1, G_2, G_3, G_4, G_5 and G_6 is 15, 25, 35, 15, 25, and 35 kHz, respectively. From the Fig. 12(a)–(c), the sideline suppression ratio for all in the spectra were better than 30 dB, this corresponds to an estimated level of crosstalk in terms of strain error of less than $1.3\mu\varepsilon$. Experiments were carried out by applying strain to G_3 and G_6 independently, the measured control voltages of the TOF corresponding to the peaks of the beat signals have good linear relations with the applied strain and no crosstalk was observed, although the two gratings are of the same beat frequency (35 kHz).

VI. Summary

In conclusion, we have demonstrated the use of a FMCW technique for addressing FBG sensor arrays. It is theoretically possible to multiplex 32 FBGs of the same nominal Bragg wavelengths with crosstalk between any two of the sensors below -48 dB. The array size could reach a few hundreds if FMCW and WDM technique are combined. In practice, the crosstalk level may be limited to be about -30 dB due to the inaccuracy in controlling the separation between the FBGs and/or the multiple reflection and spectral shadowing-related effect occurring in a serial FBG arrays. The maximum sensor number that can be multiplexed using this technique may be limited by the available source power level especially when a serial sensor array is concerned where low reflectivity FBGs have to be used in order to satisfy the crosstalk requirement. Optical amplifiers may be used to overcome the source power limitation. A three-sensor parallel FMCW FBG system with the same nominal Bragg wavelength and a six-sensor hybrid FMCW/WDM FBG system were experimentally demonstrated with -30-dB crosstalk between sensors and $2\mu\varepsilon$ strain resolution. Future work is directed on the investigation of serial-connected FMCW and hybrid FMCW/WDM FBG arrays where the spectral shadowing and multiple reflection effect would set a limit to the system performance and where the full potential of the technique may be examined.

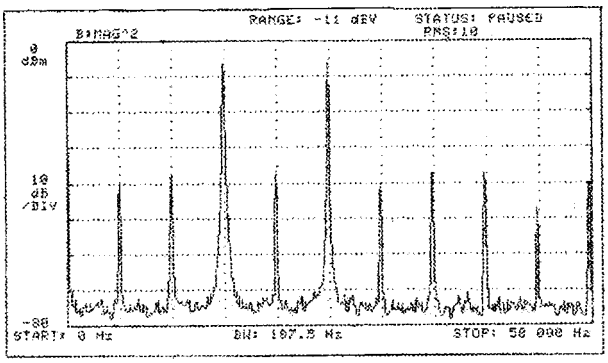

(a)

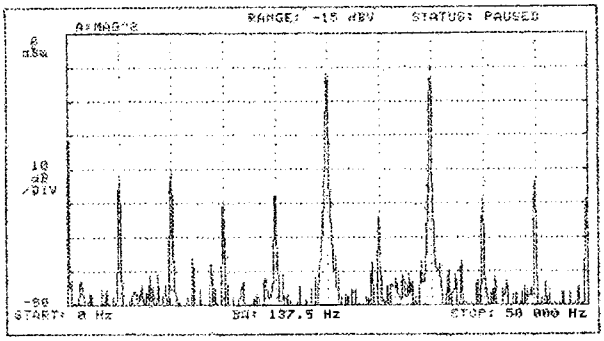

(b)

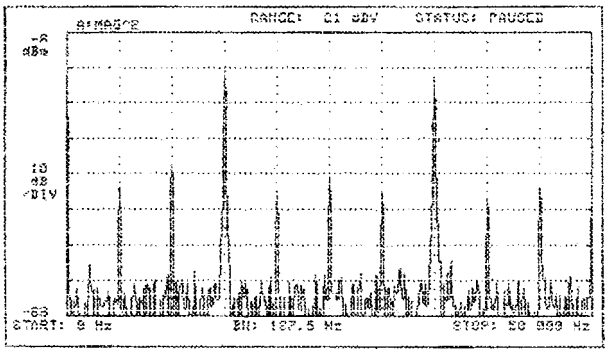

(c)

Fig. 12. Beat-note spectra of FBG sensors. (a) Signals from G_1 and G_5, (b) signal from G_2 and G_6, and (c) signal from G_3 and G_4.

REFERENCES

[1] K. O. Hill, Y. Fujii, D. C. Johnson, and B. S. Kawasaki, "Photosensitivity in optical fiber waveguides: Application to reflection filter fabrication," *Appl. Phys. Lett.*, vol. 32, pp. 647–649, May 1978.

[2] A. D. Kersey, "Interrogation and multiplexing techniques for fiber grating strain sensors," in *Proc. SPIE 2071*, 1993, pp. 30–48.

[3] Y. J. Rao, "In-fiber Bragg grating sensors," *Meas. Sci. Technol.*, vol. 8, pp. 355–375, 1997.

[4] R. L. Idriss, M. B. Kodindouma, A. D. Kersey, and M. A. Davis, "Multiplexing Bragg grating optical fiber sensors for damage evaluation in highway bridges," *Smart Material Structure*, vol. 7, pp. 209–216, 1998.

[5] M. A. Davis, D. G. Bellemore, M. A. Putnam, and A. D. Kersey, "A 60 element fiber Bragg grating sensor system," in *Proc. OFS 12th*, 1997, pp. 100–103.

[6] R. S. Weis, A. D. Kersey, and T. A. Berkoff, "A four-element fiber grating sensor array with phase-sensitive detection," *Photon. Technol. Lett.*, vol. 6, pp. 1469–1472, Dec. 1994.

[7] K. P. Koo, A. B. Tveten, and S. T. Vohra, "Dense wavelength division multiplexing of fiber Bragg grating sensors using CDMA," *Electron. Lett.*, vol. 35, pp. 165–167, 1999.

[8] K. I. Mallalieu, R. Youngquist, and D. E. N. Davies, "FMCW of optical source envelope modulation for passive multiplexing of frequency-based fiber-optic sensors," *Electron. Lett.*, vol. 22, pp. 809–810, July 1986.

[9] I. P. Giles, D. Uttam, B. Culshaw, and D. E. N. Davies, "Coherent optical-fiber sensors with modulated laser sources," *Electron. Lett.*, vol. 19, no. 1, pp. 14–15, Jan. 1983.

[10] I. P. Giles, D. Uttam, B. Culshaw, and D. E. N. Davis, "Coherent optical-fiber sensors with modulated laser sources," *Electron. Lett.*, vol. 19, pp. 14–15, Jan. 1983.

[11] I. Sakai, "Multiplexing of optical fiber sensors using a frequency-modulated source and gated output," *J. Lightwave Technol.*, vol. LT-5, pp. 932–940, 1987.

[12] A. J. Hymans and J. Lait, "Analysis of a frequency-modulated continuous-wave ranging system," *Proc. Inst. Elect. Eng.*, vol. 107B, pp. 365–372, July 1960.

[13] B. R. Mahafza, *Introduction to Radar Analysis*. Boca Raton, FL: CRC, 1998.

[14] P. J. Henderson, Y. J. Rao, and D. A. Jackson, "Simultaneous dynamic-strain and temperature monitoring using a wavelength-multiplexing fiber-Fabry–Perot array with low-coherence interrogation," in *Proc. OFS 12th*, 1997, pp. 56–59.

[15] A. D. Kersey, A. Dandridge, and K. L. Dorsey, "Transmissive serial interferometric fiber sensor array," *J. Lightwave Technol.*, vol. 7, pp. 849–854, May 1989.

[16] A. D. Kersey, M. A. Davis, H. J. Patrick, M. LeBlanc, K. P. Koo, C. G. Askins, M. A. Putnam, and E. J. Friebele, "Fiber grating sensors," *J. Lightwave Technol.*, vol. 15, no. 8, pp. 1442–1463, Aug. 1997.

[17] M. G. Xu, H. Geiger, and J. P. Dakin, "Modeling and performance analysis of a fiber Bragg grating interrogating system using an acousto-optic tunable filter," *J. Lightwave Technol.*, vol. 14, pp. 391–396, Mar. 1996.

[18] P. K. C. Chan, W. Jin, J. M. Gong, and M. S. Demokan, "Multiplexing of fiber Bragg grating sensors using an FMCW technique," *Photon. Technol. Lett.*, vol. 11, pp. 1470–1472, Nov. 1999.

Peter K. C. Chan was born in Hong Kong in 1973. He received the B.Eng. degree in electrical engineering from The Hong Kong Polytechnic University, Hong Kong, in 1996, where he is currently pursuing the Ph.D. degree in the Department of Electrical Engineering

His research interests are in the areas of multiplexing of FBG and FBG sensors for structural monitoring.

Wei Jin (M'95–SM'98) received the B.Eng. and M.Sc. degrees in control engineering from Beijing University of Aeronautics and Astronautics, Beijing, China, in 1984 and 1987, respectively, and the Ph.D. degree in fiber optics from the University of Strathclyde, Glasgow, U.K., in 1991.

From 1991 to 1995, he was a Postdoctoral Research Fellow with the Department of Electronics and Electrical Engineering, Strathclyde University. He joined the Department of Electrical Engineering, Hong Kong Polytechnic University, in early 1996 as an Assistant Professor and became an Associate Professor in early 1998. He has published 130 papers in the area of fiber optics and sensors.

Dr. Jin is a member of SPIE and OSA.

M. Süleyman Demokan (SM'89) received the B.Sc. degree in electronic engineering from the Middle East Technical University, Istanbul, Turkey, in 1970, and the M.Sc. and Ph.D. degrees, also in electronic engineering, from King's College, University of London, London, U.K., in 1972 and 1976, respectively.

From 1976 to 1983, he was with the Middle East Technical University in various capacities, including Dean of Faculty, Head of Department, and Associate Professor. After conducting research for a year at Imperial College, University of London, as a Visiting Senior Research Fellow, he joined the Hirst Research Centre of the General Electric Company, U.K., in 1984, where he directed contract research as Head of Department, Optoelectronic Components, and Chief Scientist, Optical Communications. Since 1988, he has been with The Hong Kong Polytechnic University, first as the Head of the Department of Electrical Engineering and, from 1995, as the Dean of the Faculty of Engineering. In 1992, he was conferred the title of Chair Professor of Electrical Engineering. Since 1997, he has also assumed responsibility as an Associate Vice President of the University. His current research interests include optical communication systems and fiber optic sensors.

Dr. Demokan is a Fellow of the Hong Kong Institution of Engineers and a Fellow of the Institution of Electrical Engineers.